Apollo 12 Magnetometer: Measurement of a Steady Magnetic Field on the Surface of the Moon

Abstract. *The Apollo 12 magnetometer has measured a steady magnetic field of 36 ± 5 gammas on the lunar surface. Surface gradient measurements and data from a lunar orbiting satellite indicate that this steady field is localized rather than global in its extent. These data suggest that the source is a large, magnetized body which acquired a field during an epoch in which the inducing field was much stronger than any that presently exists at the moon.*

During the first extravehicular activity of the Apollo 12 crew on 19 November 1969, a magnetometer was deployed on the eastern edge of Oceanus Procellarum as part of the Apollo Lunar Surface Experiments Package (ALSEP) (*1*). Coordinates of the magnetometer are 2.97°S and 23.35°W in the selenographic coordinate system.

The main objective of the Apollo 12 magnetometer experiment is to measure permanent and induced magnetic fields on the lunar surface. Measurements of the lunar response fields induced by time-dependent electromagnetic fields in the solar wind and earth's magnetotail permit the interior electrical properties to be calculated and an estimate of the interior lunar temperature to be made. In this report we present and discuss results from the measurement of a steady magnetic field at the Apollo 12 magnetometer site.

The magnetometer has three flux-gate sensors, which are mounted at the ends of three mutually orthogonal, 100-cm booms (see Fig. 1). In the normal operating mode the sensors are aligned along the booms, which allows each of three vector components to be measured as a function of time. When the instrument is operated as a gradiometer, the sensors are rotated such that all simultaneously align parallel first to one of the boom axes, then to each of the other two boom axes in turn. This rotating alignment allows measurement of the field gradient and also permits an independent measurement of the magnetic field vector to be made at each sensor position. The magnetometer can operate in any one of the ranges 0 to ± 100, ± 200, or ± 400 gammas with maximum frequency response from 0 to 3 hz. The electronics subsystem consists of flux-gate sensor electronics, stored digital programs for calibration and gradient operations, and a digital filter for internal data processing. Range, field offset bias, filter response, and thermal control are determined by command from earth. The mechanical subsystem of the instrument enables flipping and gimbaling of all three sensors during calibration and gradient-measurement modes. Thermal control is provided by insulation layers, control surfaces, and sensor heaters, which maintain the magnetometer within an operational temperature range of −25° to +75°C during the lunar night and day.

The magnetometer is oriented so that the *z*-axis sensor points eastward in local selenographic coordinates, and the *x* and *y* sensors point roughly northwest and southwest, respectively. The sensors are oriented at an angle of approximately 35° from the local horizontal and form an orthogonal system. The instrument is located about 125 m from the Apollo lunar module and at least 15 m from the ALSEP central station and other experiments.

Three-hour averages of magnetic field data from the first 20-day period after the instrument activation indicate a steady field of 36 ± 5 gammas at the Apollo 12 magnetometer site. The field vector is directed downward 52° from the vertical and 64° south of east, as shown in Fig. 2. Examination of the 3-hour averages and correlation with simultaneous data from the lunar orbiting satellite Explorer 35 show the steady field to be an additional feature upon which the classical solar and geomagnetic fields are superimposed. A more detailed analysis over a period of several lunations will be required to reduce the limits of uncertainty in this measurement.

The field gradient in a plane parallel to the lunar surface is less than the instrument resolution of 4 × 10^{-3} gamma per centimeter. The indication of a very low gradient and the absence of an observed field change during lunar module ascent demonstrate that the field source is not a magnetized artifact. Internal instrument calibrations have been initiated by ground commands, which have rotated the sensors through 180°, applied different field biases, and operated the gradiometer sequence. In addition, ground commands have been used to change ranges

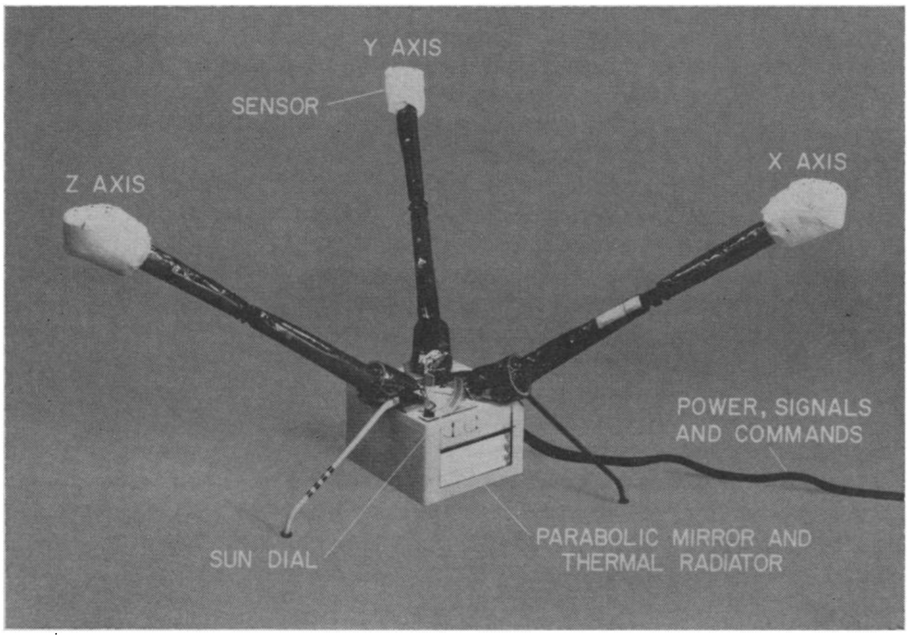

Fig. 1. Lunar surface magnetometer as deployed on the moon. The sensors are at the top end of the booms and approximately 70 cm above the lunar surface. The electronics and motor drive assembly are located in the box, encased in a thermal blanket. Heat rejection during lunar day and retention during night are controlled by a parabolic reflection array on two sides of the electronics box. The astronaut bubble level and azimuthal shadowgraph are shown on top of the box. Power, digital signals, and commands are provided through the ribbon cable, which connects to the ALSEP central station telemetry receiver and transmitter.

from $\pm$ 100 to $\pm$ 200 and $\pm$ 400 gammas in order to measure the steady field repeatedly in different instrument operational modes.

If this measured 36-gamma field were due to a dipole source located at the center of the moon, it would imply that the global magnetic moment is $M \sim 1.7 \times 10^{21}$ gauss-cm^3. Magnetometers on Explorer 35 (*2*) showed that the strength of a centered lunar dipole moment would be less than 10^{20} gauss-cm, because there was no measurable field attributable to the moon at the altitude of the satellite. It follows, therefore, that the measured 36-gamma field is due to a localized source near the Apollo 12 site. The surface Apollo 12 field intensity and gradient upper limit together with recent Explorer 35 data from orbits having periselene in the neighborhood of the ALSEP site permit the source (if assumed to be dipolar and lying near the surface) to be localized to a distance 0.2 km $\lesssim R \lesssim$ 200 km from the magnetometer and to have a magnetic moment in the range $1.4 \times 10^9 < M < 1 \times 10^{18}$ gauss-cm^3. The areal location and magnetic moment bounds indicated by the magnetic field measurements imply an extended source with remanent magnetic properties similar to those found in the Apollo 11 samples (*3*). The high coercivities and Curie temperatures of the Apollo 11 samples imply that native iron is the dominant magnetic constituent of the samples (*3*). This native iron was probably cooled below the Curie temperature at the time of the magma solidification, which was determined by the Rb/Sr dating method to have been 3.7 billion years ago (*4*).

Possible origins of such a field source include a large formation of native lunar material magnetized by an ambient field, a large magnetized meteorite, or a local region shock-magnetized by a meteorite impact. The last two hypotheses are unlikely. Analysis of Apollo 11 samples shows a low concentration of meteoritic material (*5*), which suggests that most meteorites are vaporized or melted and mixed with a relatively large amount of lunar material upon impact. Furthermore, the flooded appearance of nearby craters suggests that the crater floor materials, both meteoritic and native, have passed through the Curie temperature.

If it is assumed that the most reasonable source is magnetized native material, then one must account for the magnetizing field. In view of the high coercivity of Apollo 11 samples, such a source would have required an ambient field intensity of several times 10^3 gammas (*6*) and a mode of energy exchange in order to freeze the remanent field (*7*). This high field environment could have been due to a stronger interplanetary magnetic field, an intrinsic lunar dynamo, or a close approach to the earth. The stronger interplanetary field model is not attractive since the sector structure in the solar field would average the magnetization to a near-zero value during the long time period required for the material to cool to its Curie temperature. However, a novel solar field configuration (for example, a quadrupole) might have produced the required induction field by a combination of high solar spin and increased solar-surface field intensity. However, such an evolutionary period of the sun probably would have predated the epoch of magma solidification on the moon inferred from the Rb/Sr date.

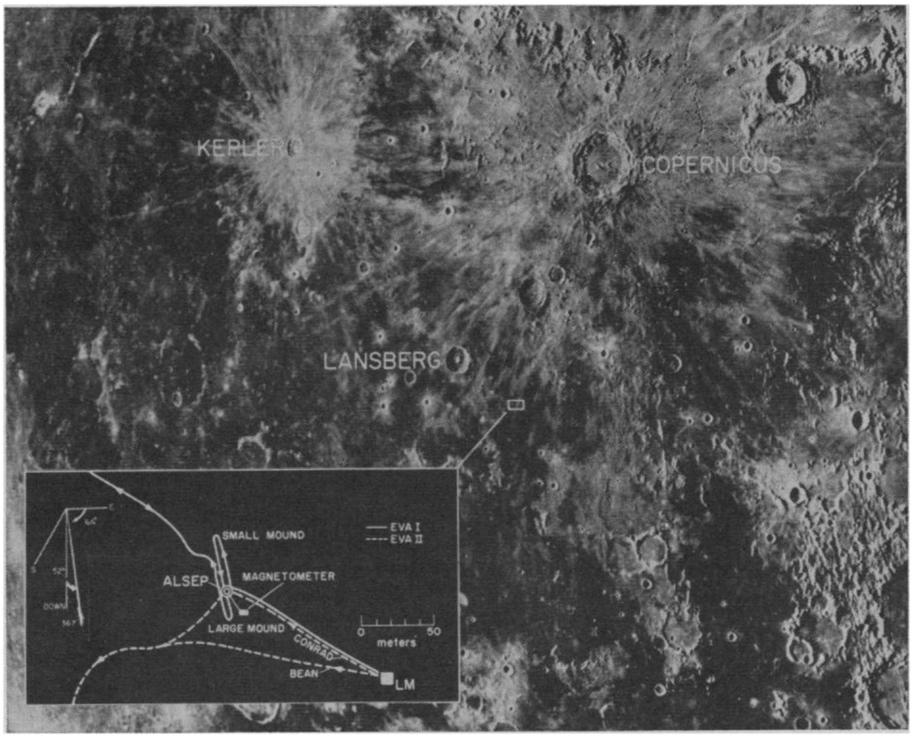

Fig. 2. Location of the Apollo 12 landing site on the moon, with an expanded view showing the location of the magnetometer and astronaut traverse. Magnetometer coordinates are 2.97°S and 23.35°W. The 36 ± 5-gamma field vector is directed downward 52° from the vertical and 64° south of east.

An intrinsic lunar dynamo requires both a hot convecting interior and a sufficient spin rate at the time the surface material is cooled below its Curie temperature. Recent theories concerning lunar rigidity require that the moon's interior be cold at present; however, the long thermal time constant of the moon precludes cooling to such a low temperature from an initial temperature hot enough to allow dynamo action. In any event, significant tidal spin degradation would have to have taken place after the material was magnetized.

An inducing field due to a close approach to earth is also possible and is consistent with the Rb/Sr isochrone of 3.7 billion years, if it is assumed that this event set the Rb/Sr "clock." In this model the hard remanence suggests a distance of closest approach of 2 to 3 earth radii, provided that the geomagnetic field at that time had the same magnitude as at present. This uncomfortable proximity to the Roche limit could be adjusted outward, however, if the geomagnetic field was larger at the time of close approach.

If the moon was magnetized by any of the mechanisms discussed here, it appears entirely possible that the anomaly at the Apollo 12 site is not unique. Thus, other higher-order contributions to the lunar field may exist and may produce a general spectrum of spatial magnetic irregularities. In such a case, the total lunar field would be dominated by wavelengths small compared with the radius of the moon and would fall off very rapidly with radial distance outward from the moon, in accordance with the lack of detectable lunar fields at the distance of the orbiting Explorer 35 satellite.

PALMER DYAL, CURTIS W. PARKIN
CHARLES P. SONETT
Space Sciences Division,
NASA Ames Research Center,
Moffett Field, California 94035

References and Notes

1. P. Dyal, C. W. Parkin, C. P. Sonett, in *Apollo 12 Preliminary Science Report* (National Aeronautics and Space Administration, Washington, D.C., in press).
2. C. P. Sonett, D. S. Colburn, R. G. Currie, *J. Geophys. Res.* **72**, 5503 (1967); N. F. Ness, K. W. Behannon, C. S. Scearce, S. C. Cantarano, *ibid.*, p. 5769; K. W. Behannon, *ibid.* **73**, 7257 (1968).
3. S. K. Runcorn, D. W. Collinson, W. O'Reilly, A. Stephenson, N. N. Greenwood, M. H. Battey, *Science* **167**, 697 (1970).
4. A. L. Albee *et al.*, *ibid.*, p. 463. Preliminary examination of the Apollo 12 samples suggests a younger age at that site on the basis of K/Ar dating; see Lunar Sample Preliminary Examination Team, *ibid.*, p. 1325.
5. K. Keil, M. Prinz, T. E. Bunch, *ibid.*, p. 597; B. Mason *et al.*, *ibid.*, p. 656.
6. C. E. Helsley, *ibid.*, p. 693.
7. R. R. Doell, C. S. Grommé, A. N. Thorpe, F. E. Senftle, *ibid.*, p. 695.
8. We thank the Apollo 12 project staff; astronauts C. Conrad, A. Bean, and R. Gordon; the ALSEP project office; and the Manned Spacecraft Center science and engineering directorates for their part in making this experiment possible. We also thank J. C. Arvesen, H. V. Cross, D. F. Engelbert, E. J. Iufer, R. M. Munoz, M. J. Prucha, and C. A. Syvertson of Ames Research Center for their decisive help. The instrument was fabricated by Philco-Ford Space and Re-entry Systems Division by a team led by C. A. Ellis. Their role under a compressed and difficult schedule was essential. We are indebted to D. S. Colburn and J. D. Mihalov for their interpretive comments and assistance in the application of correlative data from Explorer 35.

30 March 1970

Low-Velocity Zone of the Earth's Mantle: Incipient Melting Caused by Water

Abstract. *Experimental phase diagrams for the systems gabbro-water and peridotite-water indicate that, if there is any water in the upper mantle, then traces of hydrous interstitial silicate magma will be produced at depths corresponding to the beginning of the low-velocity zone. This explanation for the zone is more satisfactory than others proposed.*

Almost simultaneously with Kushiro *et al.* in 1968, we reported experimental data that suggested an explanation for the low-velocity zone in terms of incipient melting of mantle eclogite or peridotite in the presence of traces of water (*1, 2*). Anderson and Sammis and Ringwood independently deduced that incipient melting of peridotite in the presence of water was a likely explanation (*3*). The validity of this interpretation is strengthened by the recent publication of experimental data for the systems gabbro-water-carbon dioxide by Hill and Boettcher and peridotite-water by Kushiro (*4, 5*). We now consider that the model outlined below represents the most likely cause of the low-velocity zone.

The existence of a low-velocity zone in the upper mantle for most tectonic environments is now established for both *S* and *P* waves. The depth and thickness of the zone varies from one tectonic environment to another, and it is probably coincident with a layer of reduced viscosity (*6, 7*). There have been many attempts to explain this zone by departure of the geotherm from the critical temperature gradient for which the seismic velocity remains constant, or in terms of chemical or mineralogical zoning; but these explanations have not proved adequate (*3*). Many geophysicists now conclude that partial melting of the upper mantle is required to explain the observations, and the assumption has usually been implicit that melting occurred because the geotherm rose above the dry solidus. Dry melting introduces a number of problems, and it requires that the geotherm be rather sensitively controlled and constrained close to the solidus to prevent the production of too much liquid. Interpretations of the low-velocity zone in terms of partial melting of the dry mantle, and review of the problems of this interpretation, have been presented recently by Ringwood, Knopoff, Anderson, and Birch (see *3, 6, 8*).

The upper mantle contains peridotite of three types: undepleted (original), residual, and precipitated, with layers and pods of gabbro or eclogite (*9–11*). Residual peridotite may be dominant beneath the continents. According to Press, there is at least 50 percent eclogite in the suboceanic mantle between depths of 80 and 150 km (*10*). There is evidence that traces of water are present, stabilized in amphibole and phlogopite in the uppermost mantle. Superimposed on this heterogeneous mantle is a concentric succession of mineral facies. The depths to transitions between facies are sensitive to temperature variations (*9, 11*).

Addition of water to material of gabbroic composition (as shown in Fig. 1) causes depression of the melting temperatures, increases the temperature interval between solidus and liquidus, and introduces one hydrous mineral, an amphibole. The gabbro-eclogite transition interval, shown below the solidus for the dry rock, is masked by the formation of amphibole in the presence of excess water. The slope (dP/dT) of the solidus for the rock with excess water reverses at 15 kb, where plagioclase feldspar is replaced by jadeitic pyroxene (*1, 4, 12*). The hornblende-out curve for the breakdown of amphibole under these conditions also reverses slope, as predicted by Green and Ringwood and by Fry and Fyfe (*13, 14*), but our experimental data indicated that the change in slope is considerably more marked than anticipated (*2*).

This pattern of melting relationships has been confirmed by Hill and Boettcher (*4*). It is known that the hornblende-out curve extends to higher pressures and temperatures for amphiboles occurring in ultramafic rocks (*4, 15*), and to higher pressures and temperatures if water pressure is reduced compared with load pressure in the presence of a liquid phase (*4*) and in the vapor-absent region (*16*).

The solidus for dry peridotite is similar to that for gabbro in Fig. 1, and the solidus for peridotite in the presence of excess water is close to the liquids for gabbro-water in Fig. 1 (*1, 2, 4, 5*). The upper stability limit for hornblende in gabbro under these conditions thus barely overlaps the solidus for peridotite-water; Kushiro has shown that in a natural peridotite, the amphibole-out curve overlaps the solidus by a few tens of degrees within a pressure range of 8 to 17 kb (*5*).

Figure 1 is based on experiments with gabbros that become quartz eclogites at high pressures. For a gabbro undersaturated in silica to such an extent that it yielded olivine eclogite, or a simple garnet-pyroxene eclogite, we can expect that the solidus in the presence of excess water would increase in temperature rather sharply within a